

**Existence and stability of discrete gap breathers in a diatomic  $\beta$  Fermi-Pasta-Ulam chain**P. Maniadis,<sup>1,2</sup> A. V. Zolotaryuk,<sup>2,3</sup> and G. P. Tsironis<sup>2</sup><sup>1</sup>*Laboratoire Léon Brillouin (CEA-CNRS), CEA Saclay, 91191 Gif-sur-Yvette Cedex, France*<sup>2</sup>*Department of Physics, University of Crete and Foundation for Research and Technology, Hellas (FORTH), P.O. Box 2208, 71003 Heraklion, Crete, Greece*<sup>3</sup>*Bogolyubov Institute for Theoretical Physics, 03143 Kyiv, Ukraine*

(Received 5 December 2001; revised manuscript received 5 February 2003; published 21 April 2003)

We study the existence and stability of discrete breathers in a chain consisting of alternating light and heavy particles, with nearest-neighbor coupling containing quartic soft or hard anharmonicity. This study is focused on breathers with frequency in the gap that separates the acoustic and optical bands of the phonon spectrum. Simple analytical and physical results obtained through explicit solutions of algebraic equations demonstrate the possibility of the existence of gap breathers with both types of symmetry, i.e., symmetric and antisymmetric. The specific pattern depends on the type of anharmonicity present, i.e., soft or hard, and whether the center of the breather is on a light or a heavy particle. These analytical results are verified systematically through the use of a numerically exact procedure from the anticontinuous limit.

DOI: 10.1103/PhysRevE.67.046612

PACS number(s): 05.45.Yv, 63.20.Ry, 45.50.Tn, 45.90.+t

**I. INTRODUCTION**

Intrinsic localized modes or *discrete breathers* (DBs) [1–4] are nonlinear collective excitations that seem to play a very important role in condensed matter physics and even possibly in biology. Interest in these modes has been intensified recently due to their experimental generation and observation in chemical compounds [5], antiferromagnets [6], coupled arrays of Josephson junctions [7,8], and myoglobin [9]. The existence of DBs can affect essentially the physical properties of a system. Thus, as shown in Refs. [10,11], such localized vibrations are responsible for the nonexponential thermal relaxation in nonlinear lattices and therefore they are expected to contribute to the thermodynamical behavior of the system. Another physical problem, where DBs are involved, is the energy exchange between different parts of a large and complicated system. As shown by Chen *et al.* [12], under certain conditions DBs can be mobile (if they are excited appropriately) and therefore they can become energy carriers. An important property of the discrete breathers is the so-called targeted energy transfer [13], which means that under some conditions, a very selective vibrational energy transfer between DBs from one part of the system to another one can occur. Therefore, in order to understand better the importance of DBs for physical problems, it is necessary to study their fundamental properties such as their existence and stability for systems with more sophisticated (realistic) spatial symmetry and structure.

The present paper is focused on nonlinear *diatomic* lattices. Its purpose and contents are motivated as follows. Being the most simple *nonlinear* generalization of the standard one-dimensional (1D) *monoatomic* lattice with an interatomic harmonic interaction, the so-called  $\beta$  Fermi-Pasta-Ulam (FPU) chain that includes a *quartic* anharmonicity is a conventional theoretical model to describe the appearance of DBs in lattices due to discreteness and anharmonicity. As regards the symmetry of the displacements of the chain atoms from their equilibria, their profile (of the amplitudes of localized oscillations) has been shown to be either symmetric

(Sievers-Takeno mode [3]) or antisymmetric (Page mode [4]), with frequencies of oscillations shifted *above* the linear (phonon) band. A resemblance between the DBs of this type and the well known impurity modes can be described by using simple analytical calculations. The main qualitative result of such an analysis is the existence of DBs in the monoatomic  $\beta$ -FPU chain under the condition that the quartic anharmonicity is *hard*, i.e., the fourth-order expansion coefficient  $\beta$  in the interatomic interaction must be positive, if in addition the breather's higher harmonics do not resonate with frequencies from the band (a nonresonance condition [1]).

Similarly, it would be instructive to study intrinsic localized modes in a nonlinear diatomic lattice. In this paper, we consider the simplest version of the nonlinear diatomic chain that contains only nearest-neighbor interactions with a quartic (soft or hard) anharmonicity. Correspondingly, this 1D lattice can be called a diatomic  $\beta$ -FPU chain. The linear spectrum of this lattice consists of two finite bands, outside which stable DBs are expected to exist if again the nonresonance condition is fulfilled. Here we study only the breathers with frequency inside the gap separating the acoustic and optical bands. In what follows, these nonlinear localized modes are referred to as *discrete gap breathers* (DGBs).

Despite a number of disseminated publications being devoted to the existence and dynamical properties of the breathers as *strongly* localized excitations in diatomic chains [14–23], including also extended (moving) *gap solitons* [24–33], the problem of their existence and stability is not yet fully solved. In this context, Ref. [21] should be mentioned, where the DBs were investigated rigorously. However, this paper is mainly focused on the interesting bifurcation behavior of the DBs with frequency above the optical band. It should be noticed here that in order to perform the continuation of a breather solution from the anticontinuous (AC) limit in a diatomic FPU lattice, it is necessary somehow to decouple the system of nonlinearly coupled oscillators. One way to accomplish this procedure is the “freezing” of heavy masses  $M$  (the mass of light particles  $m = 1$ ), taking

the limit  $\varepsilon = M^{-1/2} \rightarrow 0$  [19,21]. In this case, a diatomic chain is continuously transformed into a monoatomic one. Below we develop another approach, which is based on an appropriate transformation of our realistic system to a fictitious lattice with its particles placed *in situ*. In other words, the equations of motion are modified to contain a *continuous* parameter, say  $\lambda$  ( $0 \leq \lambda \leq 1$ ), such that in the limit  $\lambda \rightarrow 0$ , the lattice becomes as a system of completely decoupled nonlinear oscillators, whereas in the opposite limit  $\lambda \rightarrow 1$ , the equations of motion recover their realistic (original) form. Here the AC limit corresponds to  $\lambda \rightarrow 0$ , when the intersite coupling in the system is completely transformed into a fictitious on-site potential.

The present paper aims at systematically studying the gap breather modes with all possible symmetries for both soft and hard quartic anharmonicities. In general, from symmetry arguments for each kind of anharmonicity (soft or hard), *four* possible localized solutions: centered at a light or a heavy particle with symmetric [3] or antisymmetric [4] profile may be assumed to exist. The current studies in this direction have at their disposal a powerful tool such as the MacKay-Aubry theorem [34,35] dealing with the existence and uniqueness of DBs. The numerical implementation of this theorem has recently been developed by Marín and Aubry [36], including the linear stability analysis by studying a corresponding Floquet operator. Owing to this significant progress, it is reasonable now to simplify the available analytical results concerning the breather existence (including also the previous results obtained by Aoki, Takeno, and Sievers [14], Chubykalo and Kivshar [15], and others) as much as possible, in order to get the DGB solutions in a form of closed expressions of archetypal simplicity. Therefore, using extensively symmetry arguments, here we develop a pedestrian approach. More precisely, in addition to the well known rotating wave approximation (RWA), we also introduce a local anharmonicity approximation (LAA), where the nonlinearity in the nearest-neighbor coupling is involved only for the central one (symmetric pattern) or two (antisymmetric pattern) particles of a breather profile, while the rest particles of the chain are assumed to oscillate with small amplitudes (with the harmonic approximation being applied). The LAA is reasonable, because the discrete breathers' dynamics are similar to those of impurity modes [37]. In this way, we are able to extract simplified nonlinear algebraic equations, being at the same simple level as the standard linear theory of a diatomic lattice, and at the same time giving an insight into the existence of DGBs. Thus, from our simple analysis, one can immediately show that for each type of anharmonicity (soft or hard) only *two*, instead of *four* DGB solutions, are available and find at which (light or heavy) particle their profile can be centered.

Finally, it is very important to indicate those realistic systems, where *stable* DGBs could exist. In this context, networks of hydrogen (H) bonds seem to be the most appropriate systems because their dynamics are basically governed both by nonlinearity, i.e., anharmonicity of interparticle interactions and by "diatomicity" of hydrogen bonding, i.e., the presence of two coupled species in the lattice: heavy ions and protons. More specifically, the hydrogen bonding occurs

between a proton donor group  $A-H$  and a proton acceptor group  $B$ , forming a hydrogen-bonded (HB) bridge  $A-H \cdots B$  [38]. Long chains of these bridges, like  $\cdots X-H \cdots X-H \cdots X-H \cdots$ , where  $X=A$  or  $B$  [39], are ubiquitous in soft matter; in addition to being formed in water and ice [40], they form the basic means of creating three-dimensional structures in biopolymers [41]. The typical structure of the H bond between adjacent ions  $X$  (e.g., oxygens) is that of a double well. In some cases, when the typical excitation energies are much higher or the interion distance is small, e.g., due to exogenous factors such as pressure, the H bond becomes symmetric and acquires a single well. However, in spite of the structure of realistic HB complexes being too complicated, a *soft* anharmonicity is always present in the H bond, resulting in the well-known experimental observation of decreasing the  $X-H$  stretching frequency [38]. It is thus very important to investigate thoroughly the conditions of nonlinear localization of vibrations with all possible symmetries and for all possible types of anharmonicity (soft and hard) and compare then these findings with the experiments on the redshift of the  $X-H$  frequency. Thus, the first question that immediately arises is whether or not a soft anharmonicity in the  $\beta$ -FPU model indeed results in only softening the  $X-H$  vibrations. In other words, it should be proven rigorously, using modern mathematical tools on the breather's stability, whether there exist dynamically stable localized oscillations, which bifurcate down into the frequency gap beginning from the optical band, and if this occurs, to indicate what symmetry of the oscillations is responsible for this frequency shift. The next interesting question is to examine whether or not the (nonrealistic) hard anharmonicity can participate in softening the  $X-H$  stretching vibrations. As a result of such a theoretical analysis, one can finally assert with certainty that *only one* from the *four* possible DGB's modes "survives." Its localized oscillations are proven to be symmetric and centered at a light particle (proton) in the middle of an  $X \cdots X$  bridge.

It should also be noticed that the hydrogen bonding is structurally directional and therefore except for translational motions of HB protons there are also rotations of the  $X-H$  bonds. Therefore, similarly to the existence of two types of topological solitons, i.e., extended *ionic* and *bonding* (Bjerrum) defects [42], which are related to the translational and rotational motions, respectively, two types of DBs can be distinguished in HB networks. Here we are dealing with the translational degrees of freedom in the HB chain. The existence and stability of orientational DBs in a HB chain has recently been studied by Khalack and Velgakis [43], using the AC approach.

The paper is organized as follows. In Sec. II, we introduce the model and governing equations of motion adapted for the studies, using a continuation from the anticontinuous limit. The phonon spectrum and the relation between the localization length and the gap frequency for exponentially decaying breather solutions are presented in Sec. III. The next section is devoted to an analytical analysis of all possible DGB solutions, using both the approximations: LAA and RWA. In Sec. V, we omit both the approximations and study the DGB solutions for the diatomic  $\beta$ -FPU chain, using a continuation

from the AC limit. Finally, in Sec. VI, we draw conclusions and make an outlook.

## II. MODIFIED EQUATIONS OF MOTION WITH A FICTITIOUS ON-SITE POTENTIAL

The system we study is a diatomic FPU chain with a symmetric interparticle coupling. More precisely, it is supposed that in each unit cell there exists a heavy atom (e.g., an oxygen atom with mass  $M=16$ ) and a light atom (e.g., a hydrogen atom with mass  $m=1$ ). Each atom is considered to interact only with its nearest neighbors through an anharmonic potential  $W(r)$ , where  $r$  is the relative displacement between adjacent heavy and light atoms in the chain. We consider two qualitatively different potentials  $W(r)$ , one being soft, while the other being hard.

For numerical calculations of breather states, it is essential to introduce in our system the AC limit. To this end, the nonlinear intersite potential  $W(r)$  is multiplied by a parameter  $\lambda$ , whereas each chain particle is subject to an *additional on-site potential* multiplied by some other parameter  $\eta$ . Then the AC limit is obtained if  $\lambda=0$  and  $\eta=1$ , while the original system we want to study corresponds to  $\lambda=1$  and  $\eta=0$ . The continuation from the trivial solution found in the AC limit can be implemented along any path in the two-parameter set  $(\lambda, \eta) \in [0,1] \times [0,1]$  that connects the points (1,0) and (0,1). The Hamiltonian of such a modified system takes the form

$$H = \sum_n \left[ \frac{1}{2} M \dot{Q}_n^2 + \frac{1}{2} m \dot{q}_n^2 + \lambda W(Q_n - q_n) + \lambda W(q_n - Q_{n+1}) + \eta W(Q_n) + \eta W(q_n) \right], \quad (1)$$

where the summation is over all the unit cells of the lattice and  $Q_n$  and  $q_n$  are the displacements of the heavy and light atoms in the  $n$ th cell of the chain from their equilibria, respectively. These displacements are labeled according to the sequence  $\{\dots, Q_{n-1}, q_{n-1}, Q_n, q_n, Q_{n+1}, q_{n+1}, \dots\}$ . In fact, only *one* parameter, the mass ratio  $M/m$  is characteristic for the dynamics. Nevertheless, throughout this paper we keep the symmetric notations for the masses, i.e.,  $M$  and  $m$ . In numerical simulations, we will fix  $m=1$ . For simplicity of analytical calculations, we restrict ourselves in this paper to the symmetric potential  $W(r)$ , namely,

$$W(r) = \frac{1}{2} r^2 + \frac{\beta}{4} r^4, \quad (2)$$

where the anharmonicity parameter  $\beta$  may be either positive (hard anharmonicity) or negative (soft anharmonicity).

In the simplest case, one can choose in the parameter set  $[0,1] \times [0,1]$  the straight line  $\eta = 1 - \lambda$ , so that the modified equations of motion that correspond to the Hamiltonian (1) become

$$M \ddot{Q}_n = \lambda [W'(q_n - Q_n) - W'(Q_n - q_{n-1})] - (1 - \lambda) W'(Q_n),$$

$$m \ddot{q}_n = \lambda [W'(Q_{n+1} - q_n) - W'(q_n - Q_n)] - (1 - \lambda) W'(q_n). \quad (3)$$

These equations describe the diatomic FPU chain in the AC limit if  $\lambda \rightarrow 0$ , whereas the original form of the system is obtained in the limit  $\lambda \rightarrow 1$ .

## III. DISPERSION LAWS FOR PHONONS AND DISCRETE BREATHERS

The phonon dispersion relation of a nonlinear lattice can be found if the corresponding equations of motion are linearized. Since we deal with a diatomic chain, the phonon spectrum of such a system, which can be calculated analytically, consists in general of two bands: the acoustic one with the frequencies lying between  $\omega_1$  and  $\omega_2$ , and the optical one with the frequencies lying between  $\omega_3$  and  $\omega_4$ , so that the edge frequencies for these bands are arranged as  $0 \leq \omega_1 < \omega_2 < \omega_3 < \omega_4$ . We call  $\omega_2$  and  $\omega_3$  the lower and the upper edges of the phonon band gap, respectively. In the case if the diatomic chain is isolated from any substrate (on-site) potential,  $\omega_1 = 0$ .

A necessary condition for the breather to exist is to avoid resonances with the phonons, meaning that the breather frequency and all its higher harmonics must lie outside the phonon bands. A continuation of the breather from the AC limit can be performed only if in every continuation step, the breather frequency fulfills this condition. To find a valid continuation path, it is necessary to have the phonon dispersion law for each  $\lambda$ . The corresponding linearized version of Eqs. (3) is given by

$$M \ddot{Q}_n = \lambda (q_n - 2Q_n + q_{n-1}) - (1 - \lambda) Q_n, \quad (4)$$

$$m \ddot{q}_n = \lambda (Q_{n+1} - 2q_n + Q_n) - (1 - \lambda) q_n.$$

Substituting the linear waves  $Q_n = A \exp[i(kn - \omega t)]$  and  $q_n = a \exp[i(kn - \omega t)]$ , with  $k \in [0, \pi]$  being the wave vector and  $\omega$  the phonon frequency, into the linear equations of motion (4), one can find a phonon dispersion law. As a result, the frequencies of the acoustic and optical bands as functions of the parameter  $\lambda$  are given by

$$\omega^2(k; \lambda) = \frac{1 + \lambda}{2} \left( \frac{1}{m} + \frac{1}{M} \right) \mp \sqrt{\left[ \frac{1 + \lambda}{2} \left( \frac{1}{m} - \frac{1}{M} \right) \right]^2 + \frac{2\lambda^2(1 + \cos k)}{Mm}}, \quad (5)$$

where the sign “−” (“+”) stands for the acoustic (optical) phonon band. We define the edges of these bands by

$$\omega_{1,4}(\lambda) \equiv \omega(0; \lambda) \quad \text{and} \quad \omega_{2,3}(\lambda) \equiv \omega(\pi; \lambda), \quad (6)$$

being functions of the parameter  $\lambda$ , where the subscripts “1,2” and “3,4” correspond to the signs “−” and “+.” Besides these edges, we will also use a central gap frequency defined by  $\omega_0^2 \equiv (\omega_2^2 + \omega_3^2)/2$ . On the whole interval  $0 \leq \lambda$

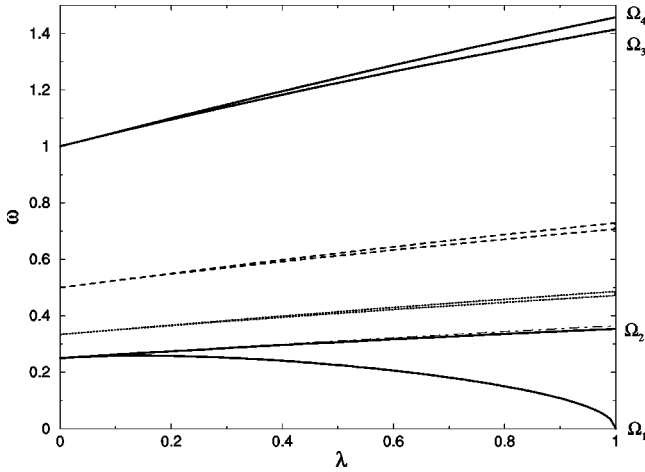


FIG. 1. Acoustic and optical phonon bands (bounded with solid lines), including the optical band divided by 2 (bounded with dashed lines), by 3 (bounded with dotted lines), and by 4 (bounded above with dotted-dashed line), plotted (in dimensionless units) as functions of the parameter  $\lambda$  for the diatomic lattice with the mass ratio  $M/m=16$ . Due to the specific value of the  $M/m$  ratio, the lower dotted-dashed line coincides with the upper edge of the acoustic band. Each of these quotient zones corresponds to breather frequencies, for which the second, third, and fourth harmonics enter the optical band. The frequencies  $\Omega_j$ 's,  $j=1,2,3,4$ , are defined by Eqs. (8).

$\leq 1$ , we have the inequalities  $0 \leq \omega_1(\lambda) \leq \omega_2(\lambda) < \omega_0 < \omega_3(\lambda) \leq \omega_4(\lambda)$ . Next, we incorporate the notations for the gap middle and the band edges at  $\lambda=1$  according to  $\Omega_j \equiv \omega_j|_{\lambda=1}$ , with  $j=0,1,2,3$ , and 4. Then one can easily obtain from Eq. (5) the following values:

$$\omega_0^2 = \frac{1+\lambda}{2} \left( \frac{1}{m} + \frac{1}{M} \right), \quad \omega_2^2 = \frac{1+\lambda}{M}, \quad \omega_3^2 = \frac{1+\lambda}{m}, \quad (7)$$

$$\Omega_1^2 = 0, \quad \Omega_2^2 = 2/M, \quad \Omega_3^2 = 2/m, \quad \Omega_4^2 = 2\Omega_0^2, \quad (8)$$

$$\Omega_0^2 = m^{-1} + M^{-1},$$

which will be used throughout this paper.

The lower and upper edges of the acoustic and optical bands are shown in Fig. 1 by solid lines for the ratio mass  $M/m=16$ . At  $\lambda=0$ , both the phonon bands merge into the two single points:  $\omega_1(0) = \omega_2(0) = M^{-1/2}$  and  $\omega_3(0) = \omega_4(0) = m^{-1/2}$ . Figure 1 also represents the three additional zones obtained from the optical band by its division by 2, 3, and 4. In order to avoid a resonance with the second harmonic, the breather frequency must lie outside the first zone bounded by the dashed lines that correspond to the lower and upper frequencies of the optical band divided by 2. Similarly, for the third harmonic, the frequency must lie outside the region bounded by the dotted lines that correspond to the lower and upper edges of the optical band divided by 3, whereas the dotted-dashed line represents the upper edge of the optical band divided by 4 (for the fourth harmonic). The fourth harmonic resonance region creates a thin zone lying very close to the acoustic phonon band from above,

which is forbidden for the breather frequency and, due to the specific mass ratio  $M/m=16$ , the lower edge of the forbidden zone coincides with the upper edge of the acoustic band (see Fig. 1). For each step in a continuation path  $\lambda = \lambda(\eta)$ , it is essential for the gap frequency  $\omega$  to lie outside the phonon bands, including the submultiples of the optical band. Thus, the frequency can lie within the gap between the optical and acoustic bands as long as its higher harmonics do not resonate with the phonons, or it can also be above the optical band. These restrictions are essential for the numerical continuation of a breather solution from the AC limit. There are many ways to get a given frequency outside the phonon bands in the limit  $\lambda \rightarrow 1$ , e.g., imposing in each step of the continuation procedure a constant distance of this frequency from a band edge.

For the localized modes, we impose an exponential decrease of the oscillation's amplitudes at  $n \rightarrow \pm \infty$  given by the exponential factor  $\exp(-|n|/\Lambda) \equiv \zeta^{|n|}$ ,  $0 < \zeta < 1$ , where  $\Lambda$  is a localization length. Since the linear waves at the frequency gap edges (i.e., at  $k = \pi$ , where  $\omega = \Omega_{2,3}$ ) become simply standing waves with out-of-phase oscillations in the neighboring lattice cells given by  $Q_n = (-1)^n A \cos(\omega t)$  and  $q_n = (-1)^n a \cos(\omega t)$ , one can assume for the DGBs the following asymptotics:

$$Q_n = (-1)^n A^\pm \zeta^{|n|} \cos(\omega t), \quad (9)$$

$$q_n = (-1)^n a^\pm \zeta^{|n|} \cos(\omega t), \quad (10)$$

as  $n \rightarrow \pm \infty$ . Here we have introduced the scaling constants (amplitudes)  $A^\pm$  and  $a^\pm$ , where the superscript “+” stands for the right asymptotics ( $n \rightarrow \infty$ ) and “-” for the left ones ( $n \rightarrow -\infty$ ). In general, the right and the left asymptotics are different, depending where and how the breather is centered. Inserting the asymptotics (9) and (10) into the linear equations of motion (4), we get the set of four linear algebraic equations with respect to the constants  $A^\pm$  and  $a^\pm$ , from which immediately one finds (at  $\lambda=1$ ) the following two relations:

$$\frac{a^\pm}{A^\pm} = \frac{\zeta^{\pm 1} - 1}{m\omega^2 - 2} = \frac{M\omega^2 - 2}{\zeta^{\mp 1} - 1}. \quad (11)$$

Here the last equality is the “dispersion law” for the gap breathers with exponentially decaying profile. The solution of this equation that depends on the parameter  $\zeta$  reads

$$\omega^2(\zeta) = \frac{1}{m} + \frac{1}{M^\mp} \sqrt{\left( \frac{1}{m} - \frac{\zeta}{M} \right) \left( \frac{1}{m} - \frac{1}{\zeta M} \right)}, \quad (12)$$

where “-” (“+”) stands for the lower (upper) branch of the curve  $\omega = \omega(\zeta)$ , with  $\Omega_2 \leq \omega \leq \Omega_0$  ( $\Omega_0 \leq \omega \leq \Omega_3$ ), plotted in Fig. 2. It is worthwhile to notice here that the imposed exponential behavior given by Eqs. (9) and (10) is also an approximation because the breather solutions of faster decrease are known at present [44].

The solution (12) is valid for the localization lengths in the interval  $[\ln(M/m)]^{-1} \leq \Lambda < \infty$ . Note also the following asymptotics that follow from Eq. (12):

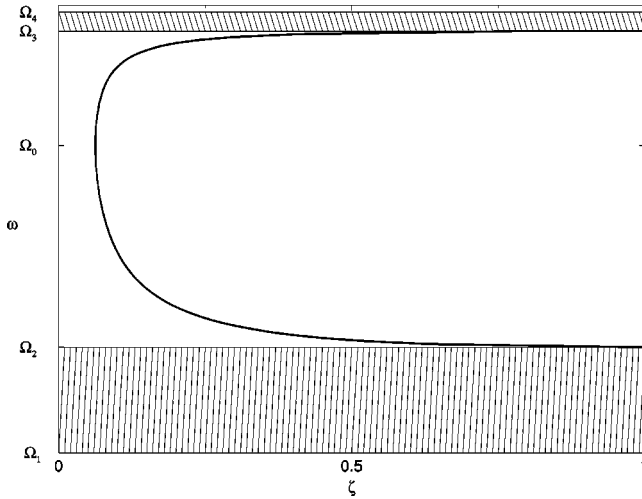


FIG. 2. Dependence of localization parameter  $\zeta$  on frequency  $\omega$  given in dimensionless units and plotted according to Eq. (14). In this figure, the edges of the phonon bands  $\Omega_1=0$ ,  $\Omega_2=0.3536$ ,  $\Omega_0=1.0308$ ,  $\Omega_3=1.414$ , and  $\Omega_4=1.4577$  are also shown.

$$M\omega^2 = 2 + \mathcal{O}[(1-\zeta)^2] \quad \text{and} \quad m\omega^2 = 2 + \mathcal{O}[(1-\zeta)^2], \quad (13)$$

at the lower and the upper gap edges, respectively. The inverse form of solution (12), which can be represented as

$$\zeta(\omega) = 1 - \frac{1}{2}(M\omega^2 - 2)(m\omega^2 - 2) - \frac{\omega}{2} \times \sqrt{(M\omega^2 - 2)(m\omega^2 - 2)[Mm\omega^2 - 2(M+m)]}, \quad (14)$$

where  $\omega \in [\Omega_2, \Omega_3]$ , will also be useful below for analytical calculations.

#### IV. LOCAL ANHARMONICITY AND ROTATING WAVE APPROXIMATIONS

The basic property of a breather solution is its spatial localization, so that only central particles in the localization region oscillate with large amplitudes, whereas the rest of the chain can be considered as linearly coupled small-amplitude oscillators. Therefore the first approximation to calculate the breather analytically is to neglect the anharmonic term in the interaction potential, except for the interaction of the central particles of the breather with its nearest neighbors. We call this approach, which is associated with the exponential ansatz given by Eqs. (9) and (10), the LAA. As a second approximation, we use for analytical calculations the well known RWA. Since we deal with potential (2), according to RWA, for the central particles of a breather ansatz in the equations of motion (3), we will make the approximate substitution:  $\cos^3(\omega t) \rightarrow (3/4)\cos(\omega t)$ .

The present section deals only with the original system, when  $\lambda = 1$ . In the LAA approach, the system of the nonlinear equations of motion [Eqs. (3) with  $\lambda = 1$ ] for the central particles is completed by the exponentially decaying solu-

tion, being an exact solution to the linear equations (4) and given by Eqs. (9)–(11), where  $\zeta$  is given by Eq. (14). Therefore below we will need to solve the nonlinear equations for the central particles of the breather centered either at a light particle or at a heavy particle, with symmetric and antisymmetric profile (using RWA), accompanying a resulting solution in each case with the linear solution given by Eqs. (9)–(11).

The following four cases of breather symmetries are possible: the breather with symmetric or antisymmetric profile is centered either at a light particle or at a heavy particle. We call each of these patterns LS and HS (when the breather with *symmetric* profile is centered at a *light* and a *heavy* particle, respectively) and LA and HA (when the breather with *antisymmetric* profile is centered at a *light* and a *heavy* particle, respectively). Below we will consider each of these cases separately.

##### A. Light-particle symmetric mode: LS pattern

The LS mode describes the breather with symmetric profile centered at a light particle, for instance, at the site with  $n=0$ . Then this particle can be assumed to oscillate with some breather frequency  $\omega$  and a certain amplitude  $a_0$ , both to be determined from the equations of motion for the central particle and its two adjacent heavy particles. The other light particles are assumed to oscillate symmetrically with the same frequency  $\omega$ , so that we suppose in Eq. (10) the symmetry  $q_{-n} = q_n$  for all  $n = \pm 1, \pm 2, \dots$ . It follows then from these conditions that in Eq. (10) one can put  $a^- = a^+ \equiv a$ . Using this symmetry property in Eqs. (11), one finds from Eq. (9) the relation  $\zeta A^+ = -A^- \equiv A$  that determines the symmetry in oscillations of the heavy particles. As a result, the LS breather ansatz can entirely be written as follows:

$$q_0 = a_0 \cos(\omega t),$$

$$q_n = (-1)^n a \zeta^{|n|} \cos(\omega t), \quad n = \pm 1, \pm 2, \dots,$$

$$Q_n = (-1)^n A \zeta^{n-1} \cos(\omega t), \quad n = 1, 2, \dots, \quad (15)$$

$$Q_n = (-1)^{n-1} A \zeta^{-n} \cos(\omega t), \quad n = 0, -1, -2, \dots$$

Schematically, the LS pattern can be represented by the sequence

$$\{ \dots; -\zeta^2 A, \zeta^2 a; \zeta A, -\zeta a; -A, a_0, -A; -\zeta a, \zeta A; \zeta^2 a, -\zeta^2 A; \dots \}. \quad (16)$$

In this sequence, the semicolons separate symmetrically the “central pattern cell” (consisting of a light particle and its two heavy neighbors) and the “lateral pattern cells” (each consisting of a light and a heavy particle, similarly to a unit cell in a diatomic chain). Note that the amplitudes in each subsequent (more remote from the center) lateral pattern cell are obtained from the amplitudes in the previous one by multiplying the latter ones by the factor  $-\zeta$ .

Next, we assume in Eqs. (3) with  $\lambda = 1$ , that only the central particle (with the coordinate  $q_0$ ) oscillates with a large amplitude  $a_0$ . In other words, we suppose that the quar-

tic anharmonicity [in potential (2)] exists only in the coupling between the central particles and its adjacent left and right heavy particles with  $Q_0$  and  $Q_1$  (using the LAA approach). The equations of motion for the central particle (situated at the site with  $n=0$ ) and one of its lateral heavy particles, e.g.,  $Q_0$  [due to the pattern symmetry,  $Q_0=Q_1=-A \cos(\omega t)$  and  $q_{-1}=q_1=-\zeta a \cos(\omega t)$ ], can be written using RWA as

$$\begin{aligned} (m\omega^2-2)a_0-2A-(3/2)\beta(a_0+A)^3 &= 0, \\ (M\omega^2-2)A-a_0+\zeta a-(3/4)\beta(a_0+A)^3 &= 0. \end{aligned} \quad (17)$$

The last two equations together with the pair of Eqs. (11) specified for the LS case as

$$\frac{a}{A} = \frac{1-\zeta^{-1}}{m\omega^2-2} = \frac{M\omega^2-2}{1-\zeta} \quad (18)$$

determine the four parameters: the amplitude of the central light particle  $a_0$ , the ‘‘amplitude scalings’’ in the heavy and light sublattices  $A$  and  $a$ , respectively, and the localization factor  $\zeta$ , as functions of the breather frequency  $\omega$  from the gap interval  $\Omega_2 < \omega < \Omega_3$ .

In order to treat the breather solution to Eqs. (17) and (18) analytically, we may assume that only the central light particle oscillates with large amplitude, whereas the amplitudes of the lateral heavy particles are small, so that they can be linearized. As a result, from Eqs. (17) and (18) one finds approximately the solution for the amplitude of the central light particle  $a_0$  in the form

$$a_0^2 = \frac{2(1+\zeta)}{3\beta\zeta \left[ \frac{1+\zeta}{1-\zeta} - \left( \frac{M}{1-\zeta} + \frac{3}{2}m \right) \omega^2 \right]} \quad (19)$$

and the relation between the amplitudes of the heavy particles and that of the central one:

$$\frac{A}{a_0} = \frac{m\omega^2-2-3\beta a_0^2/2}{2+9\beta a_0^2/2}. \quad (20)$$

The expression in the square brackets of Eq. (19) appears to be *negative* for all the gap frequencies  $\omega \in [\Omega_2, \Omega_3]$  given by Eqs. (8). This means that the LS pattern can exist only if  $\beta < 0$  (*soft* anharmonicity). Thus, the analytical solution for the LS mode as a function of the gap frequency  $\omega$  is given by Eqs. (18)–(20). More precisely, Eq. (19) determines uniquely the function  $a_0 = a_0(\omega)$ , and inserting next this function into Eq. (20), one finds the amplitude  $A = A(\omega)$ . Finally, using the function  $A(\omega)$  in any of the two equations (18), the third amplitude  $a = a(\omega)$  is easily obtained. Furthermore, all the three amplitudes  $a_0$ ,  $A$ , and  $a$  as functions of frequency  $\omega$  appear to be well defined on the whole interval  $\Omega_2 < \omega < \Omega_3$ .

Using the asymptotics (13), one can find from Eqs. (18)–(20) the asymptotic behavior of the amplitudes  $a_0$ ,  $A$ , and  $a$ , as  $\zeta \rightarrow 1$  (i.e., when the localization length  $\Lambda \rightarrow \infty$ ), approaching both the phonon bands. As a result, we obtain

$$\frac{A}{a_0} \rightarrow \frac{m}{M}, \quad \frac{a}{a_0} \rightarrow \frac{(1-\zeta)m}{2(M-m)} \quad \text{with} \quad a_0 \rightarrow 2\sqrt{\frac{-M}{3\beta(M+3m)}}, \quad (21)$$

as  $\zeta \rightarrow 1$  at the lower gap edge ( $\omega \rightarrow \Omega_2$ ), and

$$\frac{A}{a_0} \rightarrow \frac{(1-\zeta)m}{2(M-m)}, \quad \frac{a}{a_0} \rightarrow 1 \quad \text{with} \quad a_0 \rightarrow \sqrt{\frac{2(1-\zeta)m}{3\beta(m-M)}}, \quad (22)$$

as  $\zeta \rightarrow 1$  at the upper gap edge ( $\omega \rightarrow \Omega_3$ ). The LS solution given by Eqs. (18)–(20) is also simplified at the frequency  $\omega = \Omega_0$  [see Eqs. (8)], where  $\zeta = m/M$ . As a result, the LS solution at this frequency is given by the pattern (16), with

$$a_0^2 = -4M/3\beta(2M+3m), \quad A = ma_0/2M, \quad a = a_0/2. \quad (23)$$

Finally, from the comparison of the asymptotic behavior of the breather solution given by Eqs. (21) and (22) as  $\zeta \rightarrow 1$  at the lower and upper gap edges, we find that the LS breather mode bifurcates from the *optical* band. Indeed, the lower edge of the optical phonon band corresponds to the standing linear waves when the heavy particles are at rest and the light particles oscillate out of phase with the same amplitude. This phonon mode is obtained in the limit  $\zeta \rightarrow 1$  from Eqs. (22), where the amplitude  $A$  tends to zero faster than the amplitude  $a$ , and in the meantime,  $a_0 \rightarrow a$ . In other words, the local (impuritylike) negative anharmonicity causes the localization of the out-of-phase oscillations of the light particles, which in its turn results in the appearance of the localized out-of-phase oscillations of the heavy particles of the diatomic chain. Mathematically, in pattern (16), for all the frequencies from the gap interval  $\Omega_2 < \omega < \Omega_3$ , we have the inequalities:  $A > 0$  and  $a > 0$  if  $a_0 > 0$ . In spite of the LS breather solution, which is given by Eqs. (14)–(16) and (18)–(20), being obtained by using two approximations (LAA and RWA), it appears to be in a good agreement with the numerically exact solution obtained below from the AC limit when solving the equations of motion (3). The comparison of these solutions is demonstrated by Fig. 3 for two values of the breather frequency  $\omega$ . As intuitively expected, the local anharmonicity approximation should ‘‘localize’’ a little bit the influence of anharmonicity, making it effectively stronger. This is why the amplitudes  $Q_n$ 's and  $q_n$ 's obtained within this approximation appear to be a bit higher than the corresponding exact values.

## B. Heavy-particle symmetric mode: HS pattern

In the case of the HS mode, the breather is centered at a heavy ion, e.g., at the site with  $n=0$ , so that  $Q_0$  is supposed to perform large-amplitude oscillations with frequency  $\omega$  from the gap. The rest of the heavy particles of the chain are assumed to oscillate symmetrically with the same frequency:  $Q_{-n} = Q_n$  for all  $n = \pm 1, \pm 2, \dots$ . Therefore we impose in Eq. (9) that  $A^- = A^+ \equiv A$ , and using this property as well as Eq. (10), one finds from Eqs. (11) the relation  $a^+ = -\zeta a^- \equiv a$ . Let  $A_0$  be the amplitude of oscillations of the central

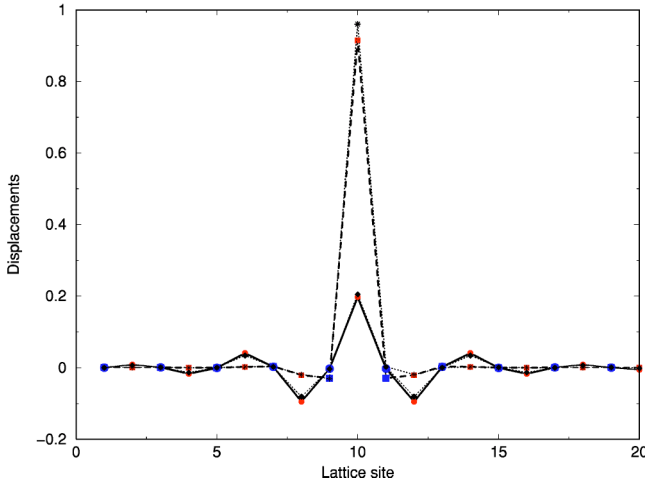


FIG. 3. The LS pattern obtained both analytically and numerically for soft interaction (2) with  $\beta = -1$  and mass ratio  $M/m = 16$ , and plotted in dimensionless units for two breather frequency values ( $\omega = 0.74$  and  $\omega = 1.40$ ). For frequency  $\omega = 1.40$ , the amplitudes  $Q_n$ 's ( $q_n$ 's) calculated numerically from the anticontinuous limit [solving the equations of motion (3)] are shown by big (small) squares connected with solid lines, whereas for frequency  $\omega = 0.74$ , these are shown by circles connected with dashed lines. Accordingly, the analytical solution given by Eqs. (14)–(16) and (18)–(20) is represented by diamonds ( $\omega = 1.40$ ) and stars ( $\omega = 0.74$ ) connected with dotted lines.

heavy particle. Then, Eqs. (9) and (10) are reduced to the following ansatz for the HS pattern:

$$Q_0 = A_0 \cos(\omega t),$$

$$Q_n = (-1)^n A \zeta^{|n|} \cos(\omega t), \quad n = \pm 1, \pm 2, \dots, \quad (24)$$

$$q_n = (-1)^n a \zeta^n \cos(\omega t), \quad n = 0, 1, \dots,$$

$$q_n = (-1)^{n+1} a \zeta^{-(n+1)} \cos(\omega t), \quad n = -1, -2, \dots,$$

which schematically can be represented in the sequence form as

$$\{ \dots; \zeta^2 a, \zeta^2 A; -\zeta a, -\zeta A; a, A_0, a; -\zeta A, -\zeta a; \zeta^2 A, \zeta^2 a; \dots \}, \quad (25)$$

where the semicolons separate symmetrically the central and the lateral pattern cells in a similar manner as in the pattern sequence (16).

It follows from the comparison of the patterns (16) and (25) that all the analytical results for the HS mode can directly be obtained from the preceding subsection by the substitution  $a_0 \rightarrow A_0$ ,  $A \rightarrow -a$ ,  $a \rightarrow A$ ,  $M \leftrightarrow m$  in the LS solution (18)–(20). As a result, instead of Eqs. (17) and (18), one obtains the system

$$(M\omega^2 - 2)A_0 + 2a - (3/2)\beta(A_0 - a)^3 = 0, \quad (26)$$

$$(m\omega^2 - 2)a + A_0 - \zeta A + (3/4)\beta(A_0 - a)^3 = 0, \quad (27)$$

$$\frac{A}{a} = \frac{\zeta^{-1} - 1}{M\omega^2 - 2} = \frac{m\omega^2 - 2}{\zeta - 1}. \quad (28)$$

Similarly, linearizing Eqs. (26) and (27) with respect to  $a$ , one finds from Eqs. (26)–(28) the following relations:

$$A_0^2 = \frac{2(1 + \zeta)}{3\beta\zeta \left[ \frac{1 + \zeta}{1 - \zeta} - \left( \frac{m}{1 - \zeta} + \frac{3}{2}M \right) \omega^2 \right]}, \quad (29)$$

$$\frac{a}{A_0} = - \frac{M\omega^2 - 2 - 3\beta A_0^2/2}{2 + 9\beta A_0^2/2}. \quad (30)$$

The HS mode is expected to bifurcate from the *acoustic* phonon band, when the light particles are at rest and the heavy particles oscillate out of phase. Similarly, as for the LS mode, one finds the asymptotics

$$\frac{a}{A_0} \rightarrow \frac{(1 - \zeta)M}{2(M - m)}, \quad \frac{A}{A_0} \rightarrow 1 \quad \text{with} \quad A_0 \rightarrow \sqrt{\frac{2(1 - \zeta)M}{3\beta(M - m)}}, \quad (31)$$

as  $\zeta \rightarrow 1$  at the lower gap edge  $\Omega_2$  [compare Eqs. (22) and (31)]. It follows from the asymptotic behavior for the amplitude  $A_0$  as  $\zeta \rightarrow 1$  that  $\beta$  must be *positive* (*hard* anharmonicity). However, contrary to the LS case [see Eq. (19)], the expression in the square brackets of Eq. (29) retains its (positive) sign only nearby the lower branch of curve (12). Therefore the HS breather solution, for which  $a > 0$  and  $A > 0$  if  $A_0 > 0$ , exists only if it is not strongly localized, in some interval  $\Omega_2 < \omega < \omega_{c,hs}$ , where the critical frequency  $\omega_{c,hs}$  is defined from zero equality of the denominator in the right hand side of Eq. (29). Thus, in the case of  $\beta = 1$ ,  $M = 16$ , and  $m = 1$ , we have  $\omega_{c,hs} = 0.3692$ . In fact, as calculated below exactly from the AC limit, the HS pattern exists for higher frequencies, e.g., for  $\omega = 0.38$  and  $\omega = 0.45$ , as illustrated by Fig. 4. The reason of this discrepancy is the same as above described for the LS pattern: due to the effective strengthening of anharmonicity, the interval of available breather frequencies  $\omega$  determined approximately by Eq. (29) becomes a bit narrower and, as a result, both the frequencies  $\omega = 0.38$  and  $\omega = 0.45$  appear outside this (approximate) interval.

### C. Light-particle antisymmetric mode: LA pattern

For the LA mode, a light particle (situated, e.g., at the site  $n = 0$ ) is fixed ( $q_0 \equiv 0$ ), whereas the rest of the light particles of the chain are allowed to oscillate antisymmetrically:  $q_{-n} = -q_n$  for all  $n = \pm 1, \pm 2, \dots$ . Therefore one may put in Eq. (10) that  $a^- = -a^+ \equiv a$ . Using then Eqs. (9) and (11), one finds that  $A^+ = -A/\zeta$  with  $-A^- \equiv A$ . Next, we assume that the two central heavy particles perform out-of-phase large-amplitude oscillations:  $Q_0 = -Q_1$ . More precisely, the LA ansatz can be written as follows:

$$q_0 \equiv 0, \quad Q_0 = -Q_1 = A_0 \cos(\omega t),$$

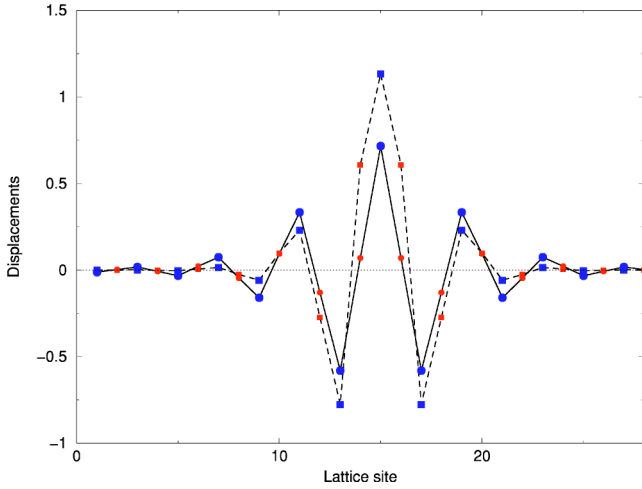


FIG. 4. The HS pattern as an exact breather solution of the equations of motion (3) for hard interaction (2) with  $\beta=1$  and mass ratio  $M/m=16$ , obtained from the anticontinuous limit. Smaller (bigger) circles or squares correspond to light (heavy) particles. The amplitudes  $Q_n$ 's and  $q_n$ 's for breather frequencies  $\omega=0.38$  (shown by circles connected with solid lines) and  $\omega=0.45$  (shown by squares connected with dashed lines) are plotted in dimensionless units.

$$q_n = \mp (-1)^n a \zeta^{|n|} \cos(\omega t), \quad n = \pm 1, \pm 2, \dots,$$

$$Q_n = (-1)^{n-1} A \zeta^{n-1} \cos(\omega t), \quad n = 2, 3, \dots, \quad (32)$$

$$Q_n = (-1)^{n-1} A \zeta^{-n} \cos(\omega t), \quad n = -1, -2, \dots$$

Schematically, this ansatz can be represented as the sequence

$$\{ \dots; \zeta^3 a, \zeta^2 A; -\zeta^2 a, -\zeta A; \zeta a, A_0, 0, -A_0, -\zeta a; \zeta A, \zeta^2 a; -\zeta^2 A, -\zeta^3 a; \dots \}. \quad (33)$$

In this sequence, the semicolons separate the central (anti-symmetric) pattern cell (consisting of a standing central light particle and its four lateral neighbors) and the lateral pattern cells (each consisting of a light and a heavy particle). Here the separation by semicolons has been arranged in a similar way as for the symmetric patterns, so that the amplitudes in each subsequent (more remote from the center) pattern cell are obtained from the amplitudes in the previous one by multiplying the latter ones by the factor  $-\zeta$ . Contrary to sequences (16) and (25), where the left and the right “wings” of the LS and the HS patterns oscillate symmetrically, here all the particles from the right and from the left of the central standing particle oscillate antisymmetrically.

Similarly to the symmetric modes studied in the previous two subsections, the approximate equations of motion for the two adjacent (heavy and light) particles [for the variables  $Q_1$  and (linearized)  $q_1$ ] take the form

$$M\ddot{Q}_1 = q_1 - 2Q_1 + \beta Q_1^2(3q_1 - 2Q_1), \quad (34)$$

$$m\ddot{q}_1 = Q_1 - 2q_1 + Q_2 + \beta Q_1^2(Q_1 - 3q_1).$$

The last two equations together with the pair of Eqs. (11) rewritten as

$$\frac{a}{A} = \frac{1 - \zeta^{-1}}{m\omega^2 - 2} = \frac{M\omega^2 - 2}{1 - \zeta} \quad (35)$$

determine the four parameters  $A_0$ ,  $a$ ,  $A$ , and  $\zeta$  as functions of the phonon gap frequency  $\omega$ . Using RWA [in Eqs. (34)] as well as Eqs. (35), we get the quadratic equation

$$\beta^2 A_0^4 + \frac{8}{9} P \beta A_0^2 - \frac{16}{27 \zeta} = 0 \quad (36)$$

with respect to  $\beta A_0^2$ , where

$$P \equiv \frac{3 - \zeta}{1 - \zeta} - \left( \frac{m}{1 - \zeta} + \frac{3}{2} M \right) \omega^2. \quad (37)$$

It is also found that the amplitude ratio is

$$\frac{a}{A_0} = - \frac{M\omega^2 - 2 - 3\beta A_0^2/2}{\zeta(1 + 9\beta A_0^2/4)}. \quad (38)$$

Since at the upper edge of the acoustic band all the heavy particles oscillate out of phase and the light particles are at rest, the LA mode (for which all the heavy particles have been assumed above to perform out-of-phase oscillations) bifurcates from the *lower* edge of the phonon gap. At the beginning of curve (12), where  $\zeta \rightarrow 1$  and therefore  $P \rightarrow 2(M-m)/(1-\zeta)M \rightarrow \infty$ , being positive, we find from Eq. (36) that  $\beta A_0^2$  must be *positive*, near this edge. Therefore the LA mode can exist only if  $\beta > 0$  (*hard* anharmonicity). More precisely, we find the following asymptotics:

$$\frac{a}{A_0} \rightarrow \frac{(1-\zeta)M}{2(M-m)}, \quad \frac{A}{A_0} \rightarrow 1 \quad \text{with} \quad A_0 \rightarrow \sqrt{\frac{(1-\zeta)M}{3\beta(M-m)}}, \quad (39)$$

as  $\zeta \rightarrow 1$ , approaching the lower gap edge. As follows from these asymptotics and sequence (33), as  $\omega \rightarrow \Omega_2$ , the amplitudes of the out-of-phase oscillations of the heavy particles are “equalized” ( $A_0 \rightarrow A$ ), while the amplitude of the light particles  $a$  tends to zero faster than the amplitude of the heavy particles  $A$ . The LA solution given by Eqs. (35)–(37) is essentially simplified at  $\omega = \Omega_0$  [see Eqs. (8)], where  $\zeta = m/M$ . Indeed, the (positive) solution of Eq. (36) is  $A_0^2 = 4M/3\beta m$  and then from Eqs. (35) and (38) we obtain  $a = M(M+m)A_0/m(3M+m)$  and  $A = (M+m)A_0/(3M+m)$ .

As regards the behavior of the amplitudes  $A_0$ ,  $a$ , and  $A$  on the whole frequency interval  $\Omega_2 < \omega < \Omega_3$ , we conclude immediately from Eqs. (35) that the signs of  $A$  and  $a$  are the same everywhere in this interval. The amplitude of the central particles  $A_0$  is given by the solution of the quadratic equation (36) with respect to  $\beta A_0^2$ , which must be positive:

$$\beta A_0^2 = - \frac{4}{9} P (\mp \sqrt{1 + 3/\zeta P^2}), \quad (40)$$

where the sign “−” stands for  $P > 0$  and “+” for  $P < 0$ , and  $\beta A_0^2 = 4/3\sqrt{3}\zeta$  if  $P = 0$ . The solution (40) monotonically increases from zero to a finite value, while running along curve (12), starting at the lower gap edge and ending at the upper one, and being positive everywhere. Using solution (40), first in Eq. (38) and then in any of Eqs. (35), we find the other amplitudes  $a$  and  $A$ . Therefore, the LA breather solution is shown to exist for all gap frequencies and no sign changes occur within the whole gap interval:  $a > 0$  and  $A > 0$  if  $A_0 > 0$ . For two breather frequencies, the approximate LA breather solution [given by the four equations (35)–(38) together with Eqs. (14) and (32) or (33)] is compared in Fig. 5 with the corresponding numerically exact solution obtained below from the AC limit by solving the equations of motion (3). In this case, the approximate solution is not so close to the exact solution as in the case of the LS pattern (compare with Fig. 3), but their qualitative agreement is still satisfactory. Note that the results obtained here for the LA mode agree (also qualitatively) with those found previously by Chubykalo and Kivshar [15].

#### D. Heavy-particle antisymmetric mode: HA pattern

For the HA pattern, a heavy particle of the chain is assumed to be fixed (e.g., at the site with  $n = 0$ , so that  $Q_0 \equiv 0$ ) and the rest of the heavy particles are imposed to oscillate antisymmetrically, i.e., in Eq. (9) we assume that  $Q_{-n} = -Q_n$ . Then we may put  $A^+ = -A^- \equiv A$ . Using next Eq. (10), from Eqs. (11) we get  $a^- = a/\zeta$ ,  $a \equiv a^+$ . Finally, we also impose the antisymmetry property for the large-amplitude oscillations of the two central light particles, assuming that  $q_0 = -q_{-1}$ . Summarizing these assumptions, Eqs. (9) and (10) can be written as the following ansatz:

$$\begin{aligned} Q_0 &\equiv 0, \quad q_{-1} = -q_0 = a_0 \cos(\omega t), \\ Q_n &= \pm (-1)^n A \zeta^{|n|} \cos(\omega t), \quad n = \pm 1, \pm 2, \dots, \\ q_n &= (-1)^n a \zeta^n \cos(\omega t), \quad n = 1, 2, \dots, \\ q_n &= (-1)^n a \zeta^{-(n+1)} \cos(\omega t), \quad n = -2, -3, \dots \end{aligned} \quad (41)$$

Schematically, this ansatz is represented by the sequence

$$\{ \dots; -\zeta^3 A, \zeta^2 a; \zeta^2 A, -\zeta a; -\zeta A, a_0, 0, -a_0, \zeta A; \zeta a, -\zeta^2 A; -\zeta^2 a, \zeta^3 A; \dots \}, \quad (42)$$

where the separation with semicolons has been arranged similarly to the LA sequence (33).

One can conclude from the comparison of the sequences (33) and (42) that all the results for the HA mode can directly be obtained from the preceding subsection by the substitution  $A_0 \rightarrow a_0$ ,  $a \rightarrow -A$ ,  $A \rightarrow a$ , and  $m \leftrightarrow M$  in the LA solution given by Eqs. (35)–(38). As a result, the corresponding relations take the form

$$\frac{A}{a} = \frac{\zeta^{-1} - 1}{M\omega^2 - 2} = \frac{m\omega^2 - 2}{\zeta - 1}, \quad (43)$$

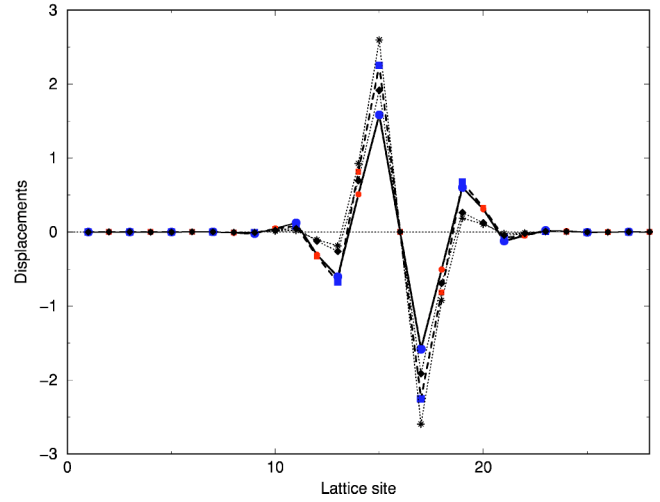


FIG. 5. The LA pattern obtained both analytically and numerically for hard interaction (2) with  $\beta = 1$  and mass ratio  $M/m = 16$ , and plotted in dimensionless units for two breather frequencies ( $\omega = 0.51$  and  $\omega = 0.63$ ). For frequency  $\omega = 0.51$ , the amplitudes  $Q_n$ 's ( $q_n$ 's) calculated numerically from the anticontinuous limit [solving the equations of motion (3)] are shown by big (small) circles connected with solid lines, whereas for frequency  $\omega = 0.63$ , these are shown by squares connected with dashed lines. Accordingly, the analytical solution given by Eqs. (14), (32), (33), (35)–(38) is represented by diamonds ( $\omega = 0.51$ ) and stars ( $\omega = 0.63$ ) connected with dotted lines.

$$\beta^2 a_0^4 + \frac{8}{9} p \beta a_0^2 - \frac{16}{27 \zeta} = 0, \quad (44)$$

$$\frac{A}{a_0} = \frac{m\omega^2 - 2 - 3\beta a_0^2/2}{\zeta(1 + 9\beta a_0^2/4)}, \quad (45)$$

where  $p$  is defined by

$$p \equiv \frac{3 - \zeta}{1 - \zeta} - \left( \frac{M}{1 - \zeta} + \frac{3}{2} m \right) \omega^2. \quad (46)$$

According to ansatz (41), all the light particles of the chain are supposed to perform out-of-phase oscillations. Since at the lower edge of the optical band, all the light particles oscillate out of phase and all the heavy particles are standing, the HA breather bifurcates from the *upper* edge of the phonon gap. At the beginning of the upper branch of curve (12) (as  $\zeta \rightarrow 1$ ),  $p \rightarrow 2(m - M)/(1 - \zeta)m \rightarrow -\infty$  [see Eq. (46)], being negative. Then, as follows from Eq. (44),  $\beta a_0^2$  must tend to zero, being *negative*. Therefore the anharmonicity must be *soft* ( $\beta < 0$ ). More precisely, we find from Eqs. (43)–(46) the following asymptotics:

$$\frac{A}{a_0} \rightarrow \frac{(1 - \zeta)m}{2(M - m)}, \quad \frac{a}{a_0} \rightarrow 1 \quad \text{with} \quad a_0 \rightarrow \sqrt{\frac{(1 - \zeta)m}{3\beta(m - M)}}, \quad (47)$$

as  $\zeta \rightarrow 1$  along the upper branch of curve (12). Since  $2/M < \omega^2 < 2/m$ , it follows from Eqs. (43) that the signs of the amplitudes  $A$  and  $a$  are the same. Therefore in the vicinity of

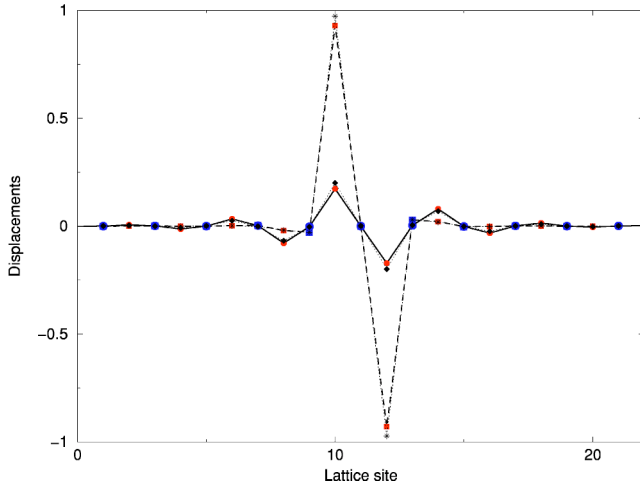


FIG. 6. The HA pattern obtained both analytically and numerically for soft interaction (2) with  $\beta = -1$  and mass ratio  $M/m = 16$ , and plotted in dimensionless units for two breather frequencies ( $\omega = 0.74$  and  $\omega = 1.40$ ). For frequency  $\omega = 1.40$ , the amplitudes  $Q_n$ 's ( $q_n$ 's) calculated numerically from the anticontinuous limit [solving the equations of motion (3)] are shown by big (small) circles connected with solid lines, whereas for frequency  $\omega = 0.74$ , these are shown by squares connected with dashed lines. Accordingly, the analytical solution given by Eqs. (14) and (41)–(46) is represented by diamonds ( $\omega = 1.40$ ) and stars ( $\omega = 0.74$ ) connected with dotted lines.

the upper gap edge, we have the inequalities  $A > 0$  and  $a > 0$  if  $a_0 > 0$ ; in fact, they can be continued on the whole curve (12). Indeed, the solution of the quadratic equation (44) for the soft anharmonicity ( $\beta < 0$ ) is given by

$$\beta a_0^2 = -\frac{4}{9}p(1 \pm \sqrt{1 + 3/\zeta p^2}), \quad (48)$$

where the sign “+” stands for  $p > 0$  and “−” for  $p < 0$ , and  $\beta a_0^2 = -4/3\sqrt{3}\zeta$  if  $p = 0$ . The solution (48) monotonically increases (in modulus) from zero to a finite value, while running along curve (12), starting at the upper gap edge and ending at the lower one. Similarly to the LS pattern, the approximate solution given by Eqs. (41)–(46) together with relation (14) is found to be in the same good agreement with the numerically exact solution obtained below from the AC limit and this is illustrated by Fig. 6.

## V. EXACT NUMERICS

So far, to treat the gap breather solutions in the diatomic chain, we have used the two approximations (LAA and RWA), and therefore we were able to get the analytical solutions for all possible symmetries in a very simple form. In this section, we will treat rigorously these breather solutions, omitting both these approximations, and study their stability using the Floquet analysis. In other words, using the approach based on the idea of the AC limit, we will calculate numerically the gap breather solutions of the original complete equations of motion (3). To this end, we choose some initial condition, starting with  $\lambda = 0$ , solve these equations

numerically using the Newton method, and then continue this procedure up to the value  $\lambda = 1$ . The continuation must proceed in a path [on the  $(\lambda, \omega)$  plane], which avoids all the resonances of the breather frequency and its higher harmonics with the phonon bands.

More precisely, for the numerical construction of DBs and the investigation of their stability, we define a vector  $\vec{X} = \{Q_1, q_1, \dots, Q_N, q_N; \dot{Q}_1, \dot{q}_1, \dots, \dot{Q}_N, \dot{q}_N\}^\dagger$ , which contains the position and the velocity of every particle in the lattice (for the numerical calculation we assume a finite lattice with  $N$  unit cells). We also define the nonlinear map  $\mathbf{T}$  that corresponds to the time evolution of the vector  $\vec{X}$  for one breather period  $t_B$ . A breather solution  $\vec{X}_B$  will correspond to a fixed point of this map [ $\vec{X}_B(t = t_B) = \mathbf{T}(\vec{X}_B(t = 0))$ ]. Assuming then that we know a vector  $\vec{X}$ , which is close to the breather solution to be found ( $\vec{X}_B = \vec{X} + \vec{\Delta}$ , where  $\vec{\Delta}$  is a vector with small magnitude) and substituting it into the previous equation, it is possible to calculate a numerically exact breather solution by solving the equation  $(\mathbf{M} - \mathbf{I}) \cdot \vec{\Delta} = \vec{X} - \mathbf{T}(\vec{X})$ , where  $\mathbf{M}$  is the tangent map of  $\mathbf{T}$  or the Floquet matrix of the system and  $\mathbf{I}$  is the unit matrix. This equation can be solved either by minimization or using the singular value decomposition. The Floquet matrix can be calculated numerically, integrating the linearized equations of motion for a small perturbation  $\vec{\epsilon}$  over one breather period  $t_B$ ,  $\vec{\epsilon}(t = t_B) = \mathbf{M} \cdot \vec{\epsilon}(t = 0)$ . The linear stability of the breather solution depends on the eigenvalues of the Floquet matrix; if one or more eigenvalues have magnitude larger than 1, then a small perturbation of the solution will grow exponentially in time and the solution will be linearly unstable. Since the Floquet matrix is symplectic (if  $\rho$  is an eigenvalue, then  $1/\rho$ ,  $\rho^*$ , and  $1/\rho^*$  are also eigenvalues), a breather is stable only if all the eigenvalues of the Floquet matrix lie on the unit circle (in the complex plane). A linearly unstable breather in a real system will be destroyed in short time due to the interactions with the environment, while a stable breather can be created spontaneously during energy relaxation, and as soon as it is created, it will have a very long lifetime. More information related to the Newton method and the stability analysis can be found in Refs. [34–36].

The continuation from the AC limit ( $\lambda \rightarrow 0$ ) is performed in the path [in the  $(\lambda, \omega)$  space], which avoids all the resonances of the breather frequency or its higher harmonics with the optical phonon band. For each step, we increase  $\lambda$  by a small quantity  $\Delta\lambda$  and then calculate the phonon frequencies from Eq. (5). If there is a resonance, we modify the breather frequency by a small quantity, in order to avoid the resonance. Then, for these specific values of  $\lambda$  and  $\omega$ , we calculate numerically the exact breather profile, using the standard Newton-Raphson method. For the next step, we increase  $\lambda$  and proceed in the same way. Below we present the results of these numerical calculations for all the four (LS, HS, LA, HA) patterns.

Thus, for the *soft* interaction potential [with  $\beta = -1$  in Eq. (2)], both the symmetric and antisymmetric modes can be found. For the symmetric mode with a light particle at the

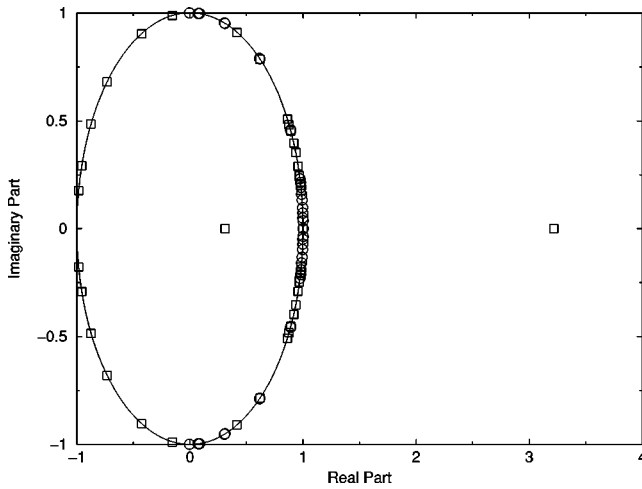


FIG. 7. Stability analysis of the breather solutions for the LS pattern. Circles and squares correspond to frequencies  $\omega = 1.40$  and  $\omega = 0.74$ , respectively.

center (LS pattern), the initial condition for the AC limit is chosen in the way when all the light and heavy particles of the chain are assumed to be at rest, except for one of the light particles, oscillating with some frequency  $\omega$  within the gap. For the antisymmetric mode with a heavy particle fixed (HA pattern), the initial condition is chosen in the way, when all the particles are supposed to stay at rest, except for two neighboring (in the light sublattice) particles, oscillating out of phase with some frequency within the gap. This mode is a multibreather with a heavy particle at rest (in the center of the multibreather) and with its nearest-neighbor light particles, oscillating out of phase.

Using the Newton method, both the LS and HA modes can be found from the AC limit for all the gap frequencies ( $\Omega_2 < \omega < \Omega_3$ ). Note, when the particle masses are  $m=1$  and  $M=16$ , we have the following values for the edges of the phonon bands:  $\Omega_1=0$  (the lower edge of the acoustic band),  $\Omega_2=0.3536$  (the upper edge of the acoustic band),  $\Omega_3=1.4142$  (the lower edge of the optical band), and  $\Omega_4=1.4577$  (the upper edge of the optical band). In Fig. 3, the amplitudes  $Q_n$ 's and  $q_n$ 's of the LS pattern are plotted for the two different frequencies, one of which is situated close to the optical band from below, while for the other frequency, the second harmonic appears to be close to the optical band, but from above. The Floquet stability analysis [see Fig. 7 with eigenvalues plotted there] shows that the LS mode is *stable* for frequencies sufficiently close to the *optical* band from *below*, and *unstable* when one of the harmonics appears sufficiently close to the *optical* band, but *above* it. The pair of Floquet eigenvalues merge into 1 on the unit circle as the frequency decreases (within the gap), beginning from the upper gap edge  $\Omega_3$ , and for a certain value, the eigenvalues collide at 1 and escape on the real axis, making the LS mode unstable. More precisely, for the mass ratio  $M/m=16$ , there exists a critical frequency, at which the breather changes its stability. The collision of the Floquet eigenvalues on the unit circle occurs at the critical frequency  $\omega_{c,ls}=0.9627$ : for breather frequencies higher than this critical value, the LS breather is stable, while for frequencies lower than the criti-

cal frequency, the LS breather is unstable. The critical velocity  $\omega_{c,ls}$  is very close to the minimum of the curve  $\zeta(\omega)$  shown in Fig. 2.

Figure 4 represents the HS pattern for two different frequencies. The first frequency lies in the gap close to the acoustic band, whereas the second one has its third harmonic, also lying in the gap, but close to the optical band. The Floquet stability analysis shows that the HS mode is unstable for each frequency within the gap. In fact, as demonstrated analytically in Sec. IV B, the interval of admissible frequencies for the HS solution is  $\Omega_2 < \omega < \omega_{c,hs} < \Omega_0$ , where  $\omega_{c,hs}$  is a critical value. As follows from the expression in the square brackets of Eq. (29), this frequency interval increases with decreasing the mass ratio  $M/m$ . Since this ratio has an integer square root equal to 4, when the frequency belongs to a thin region close to the acoustic band from above, the fourth harmonic resonates with the optical band. To avoid this resonance, we studied the case with a smaller mass ratio, namely,  $M/m=2.5$ . For this case, when the breather frequency is in the gap, all its harmonics are situated above the optical band, and therefore we avoid the resonances. The stability analysis for this mass ratio shows that the breather is *stable* only when its frequency is sufficiently close to the *acoustic* band. For larger frequencies, the breather becomes *unstable*. The critical frequency, at which the instability occurs, is  $\omega=0.9492$ , while the upper edge of the acoustic band corresponds to frequency 0.8944, so that the width of the frequency interval, where the HS breathers are stable (if  $M/m=2.5$ ), is 0.0548.

Figure 5 represents the LA pattern also for two different frequencies and the same masses  $M=16$  and  $m=1$ . In general, for any mass ratio  $M/m > 1$ , it can be found that the LA mode is *stable* if its frequency is sufficiently close to the *acoustic* band or one of its harmonics appears to lie close to the *optical* band being *above* it, and *unstable* if the frequency or one of its harmonics is sufficiently close to the *optical* band, but *below* it. Thus, for the mass ratio  $M/m=2.5$ , the stability analysis shows that there exists a critical frequency within the gap, namely,  $\omega=1.1$ , such that for all the gap frequencies larger than this value, the LA mode is unstable, whereas for all the frequencies less than this value, this mode is stable.

Figure 6 represents the HA pattern for the same frequencies as for the LS mode. This mode appears to be *unstable* for all the gap frequencies: the number of the Floquet eigenvalues that lie outside the unit circle exceeds 1. The symmetric and antisymmetric modes can also be found for potential (2) with *hard* anharmonicity, using in the same way the Newton method and the AC limit. Similarly, in this case, the symmetric mode (HS pattern) is centered on a heavy particle. The initial condition for the AC limit for this mode is chosen as follows: all the light and heavy particles are supposed to be at rest, except for one heavy particle, oscillating with some frequency within the gap. For the antisymmetric mode with a light particle fixed (LA pattern), the initial condition is chosen in the similar manner: all the particles of chain are at rest, except for two nearest-neighbor particles in the heavy sublattice, oscillating out of phase with some frequency within the gap.

TABLE I. Existence and stability results obtained by different techniques for all the four discrete gap breather modes.

Mode	Anharmonicity	Bifurcation in the gap from	Analytically approximate	Numerically exact	Stability
LS	Soft	Optical band	Within the whole gap	Within the whole gap	Stable near the optical band
HS	Hard	Acoustic band	Close to the acoustic band	Close to the acoustic band	Stable near the acoustic band
LA	Hard	Acoustic band	Within the whole gap	Close to the acoustic band	Stable near the acoustic band
HA	Soft	Optical band	Within the whole gap	Within the whole gap	Unstable within the whole gap

## VI. SUMMARY

We have examined the existence and stability of discrete breathers in an isolated diatomic chain of alternating masses coupled through potential (2) with quartic (soft or hard) anharmonicity. This chain is also called the diatomic  $\beta$ -FPU chain. The study has been performed both analytically and numerically, and restricted to the breather solutions with frequency within the gap between the acoustic and optical phonon bands. The analytical investigation has been implemented, using the two approaches: LAA and RWA. The exact breather solutions have been obtained numerically, using the AC limit. In order to apply the AC limit, the standard equations of motion for the nonlinear diatomic chain have been rewritten in terms of the parameter  $\lambda \in [0,1]$ , in such a way [see Eqs. (3)] that at  $\lambda=0$  the chain becomes a system of decoupled nonlinear oscillators, while in the limit  $\lambda \rightarrow 1$ , this decoupling is gradually removed, restoring the original (realistic) form of the chain.

For localized solutions, the LAA approach is motivated by the fact that, except for one, two, or several particles located in the center of a breather, the rest of the chain can be considered as a system of linear oscillators, admitting an exact solution with exponential behavior. The second approximation (RWA) allows us to solve analytically the nonlinear equations of motion for the central particles (where the breather is supposed to be localized) and represent the solution in simple terms. This representation is important from the point of view of the analysis of the existence of all possible types of breather solutions with given soft or hard anharmonicity in potential (2). Thus, using the structure of the phonon modes at the upper edge of the acoustic band (light masses are at rest, while heavy masses oscillate out of phase) and the lower edge of the optical band (heavy masses are at rest, while light masses oscillate out of phase), we are able to derive the four ansätze that correspond to all possible symmetries of the breather patterns, with Sievers-Takeno-like symmetric [3] and Page-like antisymmetric [4] profiles in each (light and heavy) sublattice. As a result, we have obtained *simple algebraic* expressions in terms of a finite number of amplitude parameters. The minimal number of these amplitudes for any type of breather solutions, LS, HS, LA, or HA is three:  $a_0$  or  $A_0$ ,  $a$ , and  $A$ . These three amplitudes together with the parameter  $\zeta$  satisfy in each case the system of four algebraic equations: Eqs. (18)–(20) for the LS mode, Eqs. (28)–(30) for the HS mode, Eqs. (35)–(38) for the LA mode, and Eqs. (43)–(46) for the HA mode. As illustrated in Figs. 3, 5, and 6, the agreement of these *analytically approximate* breather solutions with the corresponding *numerically*

*exact* solutions found from the AC limit by solving the equations of motion (3) appears to be relatively good. Here the analytical values for the amplitudes  $Q_n$ 's and  $q_n$ 's are higher than their corresponding exact values. This is because the local anharmonicity approximation effectively strengthens the influence of anharmonicity, making it effectively stronger and resulting in strengthening the localization.

In each case (soft or hard anharmonicity), *two*, instead of four, breather solutions have been shown to exist (analytically and confirmed numerically): LS and HA for soft anharmonicity, and HS and LA for hard anharmonicity. Three of these modes (LS, LA, and HA) exist for any frequency in the gap, while the HS mode can exist only near the lower gap edge. All these results are qualitatively summarized in Table I. Since the hydrogen bonding has a *soft* anharmonicity, it follows from this table that only the LS pattern is appropriate. This pattern describes the infrared shift of vibrational spectra observed in numerous experiments.

As follows from the breather solutions plotted in Figs. 3–6, in each pattern cell [in the sequences (16), (25), (33), and (42), the pattern cells are separated with semicolons] of the LS and HA modes, the *light* and *heavy* particles oscillate being displaced in *opposite* directions, whereas these displacements occur in the *same* directions for the HS and LA breathers. This different dynamical behavior is because of inertia in high-frequency oscillating motion: it is easier for a light particle to follow a heavy one than vice versa.

The Floquet stability analysis of all these patterns has shown that when we avoid the nonresonance condition, only the HA mode is unstable for all the gap frequencies. This instability comes from the fact that the HA mode is a multi-breather, centered at a heavy particle at rest, with its nearest-neighbor light particles oscillating out of phase. In physical terms, the stability of the LA mode can be understood when its profile is compared with the stable Page mode [4] for a monoatomic chain: light masses are easily drawn into the oscillating motion and they do not perturb strongly the motion of heavy masses.

## ACKNOWLEDGMENTS

The work was partially supported by the European Union under INTAS Grant Nos. 96-0158 and 97-0368 and RTN Grant No. HPRN-CT-1999-00163. The authors are grateful to S. Aubry and J. M. Khalack for helpful discussions and valuable suggestions, which have resulted in an essential improvement of the present paper.

- [1] For a review see, e.g., S. Flach and C.R. Willis, *Phys. Rep.* **295**, 181 (1998).
- [2] A.A. Ovchinnikov, *Zh. Eksp. Teor. Fiz.* **57**, 263 (1969) [*Sov. Phys. JETP* **30**, 147 (1970)]; A.M. Kosevich and A.S. Kovalev, *ibid.* **40**, 981 (1974) [*Sov. Phys.* **67**, 1793 (1974)].
- [3] A.J. Sievers and S. Takeno, *Phys. Rev. Lett.* **61**, 970 (1988).
- [4] J.B. Page, *Phys. Rev. B* **41**, 7835 (1990).
- [5] B.I. Swanson, J.A. Brozik, S.P. Love, G.F. Strouse, A.P. Shreve, A.R. Bishop, W.-Z. Wang, and M.I. Salkola, *Phys. Rev. Lett.* **82**, 3288 (1999).
- [6] U.T. Schwarz, L.Q. English, and A.J. Sievers, *Phys. Rev. Lett.* **83**, 223 (1999).
- [7] E. Trias, J.J. Mazo, and T.P. Orlando, *Phys. Rev. Lett.* **84**, 741 (2000).
- [8] P. Binder, D. Abraimov, A.V. Ustinov, S. Flach, and Y. Zolotaryuk, *Phys. Rev. Lett.* **84**, 745 (2000).
- [9] A. Xie, L. van der Meer, W. Hoff, and R.H. Austin, *Phys. Rev. Lett.* **84**, 5435 (2000).
- [10] G.P. Tsironis and S. Aubry, *Phys. Rev. Lett.* **77**, 5225 (1996).
- [11] A. Bikaki, N.K. Voulgarakis, S. Aubry, and G.P. Tsironis, *Phys. Rev. E* **59**, 1234 (1999).
- [12] D. Chen, S. Aubry, and G.P. Tsironis, *Phys. Rev. Lett.* **77**, 4776 (1996).
- [13] G. Kopidakis, S. Aubry, and G.P. Tsironis, *Phys. Rev. Lett.* **87**, 165501 (2001).
- [14] M. Aoki, S. Takeno, and A.J. Sievers, *J. Phys. Soc. Jpn.* **62**, 4295 (1993).
- [15] O.A. Chubykalo and Y.S. Kivshar, *Phys. Rev. E* **48**, 4128 (1993); **49**, 5906 (1994).
- [16] S.A. Kiselev, S.R. Bickham, and A.J. Sievers, *Phys. Rev. B* **48**, 13 508 (1993); **50**, 9135 (1994).
- [17] M. Aoki and S. Takeno, *J. Phys. Soc. Jpn.* **64**, 809 (1995).
- [18] G. Zhou, Y. Duan, and J. Yan, *Phys. Rev. B* **53**, 13 977 (1996).
- [19] R. Livi, M. Spicci, and R.S. MacKay, *Nonlinearity* **10**, 1421 (1997).
- [20] S.A. Kiselev, R. Lai, and A.J. Sievers, *Phys. Rev. B* **57**, 3402 (1998).
- [21] T. Cretegnny, R. Livi, and M. Spicci, *Physica D* **119**, 88 (1998).
- [22] M. Hörnquist, E. Lennholm, and C. Basu, *Physica D* **136**, 93 (2000).
- [23] A.V. Zolotaryuk, P. Maniadis, and G.P. Tsironis, *Physica B* **296**, 251 (2001).
- [24] St. Pnevmatikos, N. Flytzanis, and M. Remoissenet, *Phys. Rev. B* **33**, 2308 (1986).
- [25] Y.S. Kivshar and N. Flytzanis, *Phys. Rev. A* **46**, 7972 (1992).
- [26] Y.S. Kivshar, *Phys. Rev. Lett.* **70**, 3055 (1993).
- [27] O.A. Chubykalo, A.S. Kovalev, and O.V. Usatenko, *Phys. Rev. B* **47**, 3153 (1993).
- [28] G. Huang, *Phys. Rev. B* **51**, 12 347 (1995).
- [29] Y.S. Kivshar, O.A. Chubykalo, O.V. Usatenko, and D.V. Grinyoff, *Int. J. Mod. Phys. B* **9**, 2963 (1996).
- [30] A.S. Gorshkov, O.N. Ermakova, and V.F. Marchenko, *Nonlinearity* **10**, 1007 (1997).
- [31] G. Huang and B. Hu, *Phys. Rev. B* **57**, 5746 (1998).
- [32] A.S. Kovalev, O.V. Usatenko, and A.V. Gorbach, *Phys. Rev. E* **60**, 2309 (1999).
- [33] B. Hu, G. Huang, and M.G. Velarde, *Phys. Rev. E* **62**, 2827 (2000).
- [34] R.S. MacKay and S. Aubry, *Nonlinearity* **7**, 1623 (1994).
- [35] S. Aubry, *Physica D* **71**, 196 (1994); **103**, 201 (1996).
- [36] J.L. Marín and S. Aubry, *Nonlinearity* **9**, 1501 (1994).
- [37] P. Maniadis (unpublished).
- [38] For details see, e.g., S.N. Vinogradov and R.H. Linnell, *Hydrogen Bonding* (Van Nostrand Reinhold Company, New York, 1971); G.A. Jeffrey, *An Introduction to Hydrogen Bonding* (Oxford University Press, New York, 1997).
- [39] For a review see, e.g., J.F. Nagle and S. Tristram-Nagle, *J. Membr. Biol.* **74**, 1 (1983).
- [40] P.V. Hobbs, *Ice Physics* (Clarendon, Oxford, 1974).
- [41] L. Stryer, *Biochemistry* (W. H. Freeman and Company, New York, 1995).
- [42] See, e.g., St. Pnevmatikos, G.P. Tsironis, and A.V. Zolotaryuk, *J. Mol. Liq.* **41**, 85 (1989).
- [43] J.M. Khalack and M.J. Velgakis, *Phys. Rev. E* **65**, 046604 (2002).
- [44] M. Eleftheriou, B. Dey, and G.P. Tsironis, *Phys. Rev. E* **62**, 7540 (2000).